crystals

MDPI

Review

Artificial Intelligence and Li Ion Batteries: Basics and Breakthroughs in Electrolyte Materials Discovery

Haneen Alzamer, Russlan Jaafreh, Jung-Gu Kim * and Kotiba Hamad *

School of Advanced Materials Science, Engineering Sungkyunkwan University, Suwon 16419, Republic of Korea
* Correspondence: kimjg@skku.ac.kr (J.-G.K.); hamad82@skku.edu (K.H.)

Abstract: Recent advancements in artificial intelligence (AI), particularly in algorithms and computing power, have led to the widespread adoption of AI techniques in various scientific and engineering disciplines. Among these, materials science has seen a significant transformation due to the availability of vast datasets, through which AI techniques, such as machine learning (ML) and deep learning (DL), can solve complex problems. One area where AI is proving to be highly impactful is in the design of high-performance Li-ion batteries (LIBs). The ability to accelerate the discovery of new materials with optimized structures using AI can potentially revolutionize the development of LIBs, which are important for energy storage and electric vehicle technologies. However, while there is growing interest in using AI to design LIBs, the application of AI to discover new electrolytic systems for LIBs needs more investigation. The gap in existing research lies in the lack of a comprehensive framework that integrates AI-driven techniques with the specific requirements for electrolyte development in LIBs. This research aims to fill this gap by reviewing the application of AI for discovering and designing new electrolytic systems for LIBs. In this study, we outlined the fundamental processes involved in applying AI to this domain, including data processing, feature engineering, model training, testing, and validation. We also discussed the quantitative evaluation of structure–property relationships in electrolytic systems, which is guided by AI methods. This work presents a novel approach to use AI for the accelerated discovery of LIB electrolytes, which has the potential to significantly enhance the performance and efficiency of next-generation battery technologies.

Keywords: Li-ion batteries; electrolytes; AI; machine learning; deep learning

check for updates

Academic Editor: Faxing Wang

Received: 16 December 2024
Revised: 17 January 2025
Accepted: 18 January 2025
Published: 23 January 2025

Citation: Alzamer, H.; Jaafreh, R.; Kim, J.-G.; Hamad, K. Artificial Intelligence and Li Ion Batteries: Basics and Breakthroughs in Electrolyte Materials Discovery. *Crystals* **2025**, *15*, 114. https://doi.org/10.3390/cryst15020114

Copyright: © 2025 by the authors. Licensee MDPI, Basel, Switzerland. This article is an open access article distributed under the terms and conditions of the Creative Commons Attribution (CC BY) license (https://creativecommons.org/licenses/by/4.0/).

1. Introduction

Recently, there has been growing interest in the materials discovery process to find new combinations with specific targeted properties, and this should be achieved by reducing the number of costly and time-consuming trial and error experiments [1]. For example, to find the optimized composition of a thermoelectric material that can result in a high value of the figure of merit (ZT) [2], one might need to conduct a large number of costly and time-consuming experiments. The same example is applied for the various types of advanced materials that are used for energy harvesting and storage applications [3]. Generally speaking, experimental measurements, which usually include microstructure and property analysis, property measurement, synthetic experiments, and so on, is an easy and intuitive method of materials research, although it is usually conducted in an inefficient manner over a long time period. Alternatively, computational simulation, ranging from electronic structure calculations based on density functional theory (DFT), molecular dynamics (MD), Monte Carlo techniques, and the phase-field (PF) method to continuum macroscopic

approaches, is another approach in which existing theories are exploited for analysis using computer programs [4]. In addition, computational methods can give a further understanding of the material's fundamentals, because they can be used to simulate behaviors at the atomic level. Although those methods are more effective when compared to experimental procedures in terms of time and cost, their performance still needs to be improved, especially when many experimental parameters are to be considered. Up to this end, the AI techniques (machine learning and deep learning (ML&DL)) were found to be very successful in achieving this target in materials science, where such statistical methods were used to predict molecular properties, transition states, dielectric constant, and band gaps [5]. AI techniques play a particularly important role due to their ability to learn behaviors and trends present within the periodic table and make predictions based on the learned trends. This was additionally motivated by the various rapid improvements in ML algorithms and the exponential growth in computing power. Using these methods, discovering new materials provides many benefits that can complete the experimental-based materials discovery [6–8]. Considering the great development achieved in the field of learning algorithms and the deep understanding of their techniques, there will be many and several opportunities for further breakthroughs in the field of automated discovery and the design of advanced energy materials using AI. For example, materials included as active components in thermoelectric devices for thermal energy harvesting need to possess low thermal conductivity [9–11]. In this application, searching for such materials based on conventional methods, like physics-based simulations (DFT and MD) and trial-and-error studies, is a quite expensive and time-consuming process, and to overcome these limitations, ML&DL-based design loops were introduced in several works [10].

Another example dealing with the same issue is the implantation of such techniques to optimize the performance and safety of Li-ion batteries (LIBs) [12–16], where the applications of learning techniques in LIBs-related research can be indicated by the exponential growth of publication numbers, as shown in Figure 1a. These techniques were employed in various directions to achieve this target of high performance. For instance, electrolytic systems with high ionic conductivity, low electronic conductivity, and improved electrochemical stability could be designed through learning techniques [12]. In the present review, the recent advances achieved within this area will be discussed in detail, and this can serve as an important source to the LIBs research community and encourage them to integrate AI into their research activities.

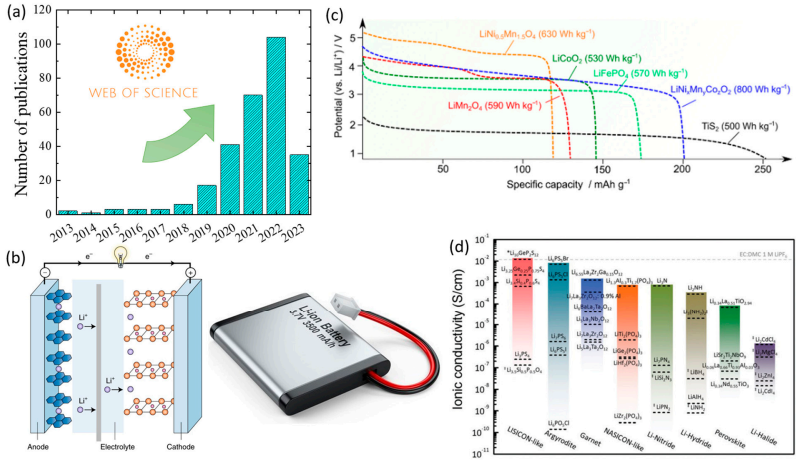

Figure 1. (**a**) The progress in the field of AI-guided Li batteries between 2013 and 2023, as reported by the Web of Science. (**b**) Components of a rechargeable Li-ion battery. (**c**) The performance of several cathodic materials in LIBs [14]. (**d**) The performance of several traditional solid electrolytes used in LIBs [14]. Adapted with permission from Ref. [14].

2. Why Are Learning Techniques Needed in Li-Ion Batteries?

The need for rechargeable batteries was started by the invention of portable electronic devices, where LIBs showed more potential in these applications than other secondary batteries, such as Ni metal hydride and lead–acid [17–19]. They show energy density of ~150 W/Kg, which is three to five times higher than that of their Ni metal hydride and lead–acid counterparts. That is mainly due to the superior energy density of the LIBs compared to other systems in the market, which is, in turn, related to the organic electrolytes that can secure a wide voltage window and high reduction potential of Li combined with its low atomic mass and volume. Originally, thinking about this type of battery was initiated in 1913 by Lewis and Keyes [20], who designed a Li-metal battery (LMB). Then, in 1965, Selim et al. at NASA attempted to use a lithium metal anode in a propylene carbonate-based electrolyte, which is a more familiar configuration of lithium-ion batteries [21]. However, they expressed practicality concerns due to the low stripping/redeposition efficiency, where it was found that only about 50–70% of the lithium ions were able to be effectively removed from and redeposited onto the lithium metal anode during the charging and discharging cycles. The path to commercialize the LIBs basically started through looking for electrode materials (cathode and anode) that optimize the performance of the battery. For example, the search was focused initially on finding anodes that are safer and more stable than pure Li. In this regard, the development of LIBs technology achieved a significant breakthrough when lithium metal, as the anode active material, was replaced with carbonaceous compounds, predominantly graphite, in modern-day LIBs [22]. In addition, a huge amount of research was conducted to find suitable cathode materials that are stable, cheap, and possess high specific capacity to be used in commercial LIBs. In fact, the majority of LIBs available in the market employ a mixture of lithium transition metal oxides (LMOs) such as $LiNiO_2$ and $LiCoO_2$ as cathode materials. By carefully adjusting the mixture, the energy density, stability, safety, and cost can be balanced to meet the requirements of the specific application (Figure 1). Optimizing the performance of lithium-ion batteries also requires addressing the issue of electrolyte materials. In the current design, a liquid organic solution is utilized as a Li-ion conducting electrolyte, where this solution consists of lithium hexafluorophosphate ($LiPF_6$) as a conducting salt and a mixture of organic solvents, such as dimethyl carbonate and methyl carbonate [14]. This mixture can offer several advantages that contribute to enhance the performance of the battery during the applications, like an ionic conductivity of ~10^{-2} S/cm, which is sufficient to allow efficient ion transport between the cathode and anode during the charge and discharge cycles of the battery. This is related to the low dissociation energy of $LiPF_6$ and its excellent solubility in the organic solution. In addition, the presence of fluoride in the $LiPF_6$ enhances its stability toward oxidation, and thus it can be used safely with positive electrodes that have potential >4 V [18]. Even though such electrolyte materials perform well in the commercialized LIBs, new materials are always requested to meet the needs of new devices. For example, in high-temperature applications (>60 °C), $LiPF_6$ undergoes thermal decomposition, leading to a reduction in the performance of the battery, and accordingly, these materials must be replaced with more thermally stable candidates. Up to here, the search for new materials that can improve the performance of LIBs is a large area in energy-related research [23]. For example, due to the low thermal stability of the conventional liquid electrolyte, academic and industrial research are focused on the employment of solid-state electrolytes, which offer higher stability compared to their liquid state counterpart. On the other hand, the new solid-state candidate must possess high ionic conductivity, which needs to be close to that in the liquid electrolyte (~10^{-2} S/cm), and this should be conjugated with low electronic conductivity and high chemical stability [24]. Reaching an electrolyte composition with these characteristics based on traditional methods used

in materials design is an exhausting task and needs a lot of resources. Here, a promising approach to tackling this challenge lies in the application of learning techniques (machine and deep learning). By employing the learning techniques, large datasets containing information on the structure, composition, and properties of various materials can be analyzed, thereby identifying patterns, correlations, and trends that may not be readily apparent to human researchers. Through this data-driven approach, learning techniques enable the prediction and optimization of electrolytic material properties, including high ionic conductivity, low electronic conductivity, and high chemical stability, which are crucial for solid-state electrolytes in LIBs.

Up to this end, learning techniques can be applied to optimize the battery's components, such as electrodes and electrolytes, to enhance the battery's overall performance. For instance, machine learning algorithms can be used to predict the performance of different electrode [25–64] and electrolyte materials [65–90], enabling researchers to select the most promising materials for further investigation. This approach can lead to the development of new and improved battery components that exhibit better performance, stability, and safety. In addition, performance monitoring, which involves tracking the battery's state-of-health (SoH) during its usage to ensure optimal performance and to prevent premature failure, can be guided by AI techniques [91–138]. SoH measurements can include analyzing the capacity, voltage, temperature, and internal resistance of the battery. By continuously monitoring such parameters, any anomalies or deviations can be identified and addressed before they result in permanent damage to the battery.

3. Basics of Learning Producer

3.1. Learning Data

To construct a predictive learning model aimed at optimizing the components of LIBs to enhance their performance, the initial dataset plays a fundamental role as the cornerstone of this process. The availability of data is imperative, as it serves as the foundation upon which the model is built. It provides the necessary information and insights that enable the model to learn, generalize, and make predictions about the behavior and characteristics of different LIB components. Without a robust and diverse dataset, the model lacks the necessary information to accurately understand the underlying patterns and relationships within the data. In this regard, collecting enough data is the first step in the learning process, and here, two different cases are distinguished. Firstly, when aiming to predict and optimize a specific property (Y) in materials for targeted applications, such as hardness, it is necessary to have an initial dataset that includes the property (Y) for a substantial number of materials. For example, when the target is to discover new super-hard materials, the information of super-hard materials (hardness, compositions, and processing conditions) needs to be collected for as many as possible cases [139]. Through the learning process, a model can be developed to establish the relationship between hardness, materials composition, and processing conditions. This model can then be utilized to design novel super-hard materials based on the knowledge derived from the initial dataset. Alternatively, in certain scenarios, there may be a lack of direct property data available for a sufficient number of materials under consistent conditions. In such cases, a proxy is employed instead of the direct property to construct the learning model, and typically, this proxy exhibits a specific correlation with the primary property of interest in the material. On example here is to use the shear modulus-to-bulk modulus ratio (G/B) as a proxy to predict the brittle–ductile behavior of crystalline solids according to the Pugh's criterion [140,141]. This is due to the insufficient amount of data on the direct property (brittle-ductile behavior) for an adequate number of crystalline solids, whereas measurements related to G and B are often available for a large variety of materials. The G/B ratio served as a suitable

substitute, enabling the construction of the learning model that could be used to predict the structure of ductile perovskite materials [140]. This approach can also be employed in a transfer learning process, where the knowledge gained from a large dataset using a proxy is transferred to a model focused on the direct property using a smaller dataset. To illustrate, consider the case of predicting the thermal conductivity of polymers with a limited dataset. In this scenario, the glass transition temperature (T_g) of polymers, which has a large dataset available, can be utilized as a proxy. Through transfer learning, the insights and patterns learned from the T_g dataset can be effectively transferred to build a model that predicts the thermal conductivity of polymers despite the smaller dataset available for this specific property.

Up to here, it will be worth discussing the various sources of data to be involved in learning processes. Typically, when an AI expert is asked about the required size of data, the response is often along the lines of "as many cases as possible". However, in AI-related materials science and engineering research, the availability of data is an issue. In this context, the initial approach involves creating an in-house dataset by conducting new experiments within the desired range of compositions and properties. For example, Xue et al. [142] prepared 50 TiNi-based shape memory alloys and measured their transformation temperature as the targeted property. This small size dataset was then employed in a learning process to build a model that relates composition and transformation temperature in this type of shape memory alloy (Figure 2). However, due to the limited size of the dataset, this model was not effectively leveraged to identify new alloys with optimized properties. The small dataset size significantly hinders its ability to generalize and make accurate predictions across a broader range of compositions.

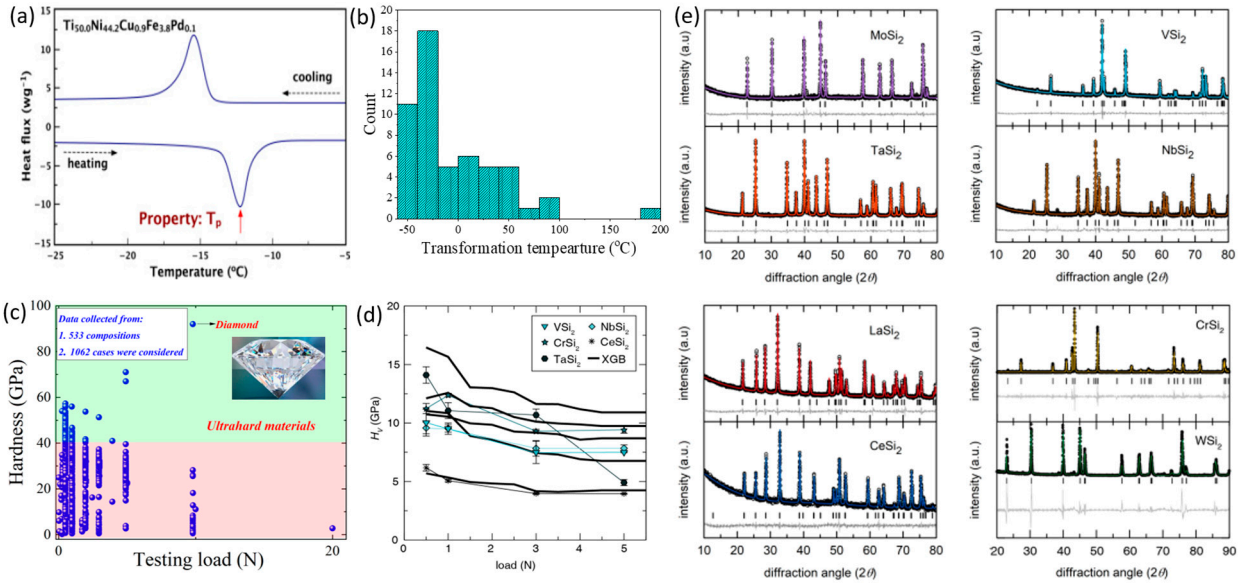

Figure 2. (**a**) The optimization of the endothermic peak observed in the differential scanning calorimetry (DSC) curve, denoted as ΔH, as reported by Xue et al. [142] (**b**) The histogram of the transformation temperature as reported by Xue et al. [142] (**c**) The Vickers hardness vs. testing load correlation of the initial dataset of the work conducted by Zhang et al. [139] (**d**) The experimental vs. predicted Vickers hardness comparison as a function of the load handled by the XGB ensemble learning technique. (**e**) Enhancement of X-ray powder diffraction data for disilicides M Si_2 (M = Mo, Ta, V, Nb, La, Ce, Cr, and W) by Zhang et al. [139]. Adapted with permission from Ref. [139].

In order to extend the dataset and achieve a more accurate and generalized model, previous works conducted on the same topic can be used to extract needed data for the learning process. For example, for designing new super-hard materials (40 GPa), a

dataset containing the information of ~530 materials (hardness, load, and compositions) was extracted from works reported on the preparation and characterization of super-hard materials (Figure 2) [139]. Indeed, a learning model with high accuracy (~97%) was built and used to predict the composition of new super-hard materials. This model was additionally validated through an experimental work, where five compositions MSi_2 (M = V, Nb, Cr, Ce, and Ta) were prepared, and their measured harness was compared to that of the predicted counterpart (Figure 2). Data extracted from other studies were employed in various works, such as design steel and Al alloys with improved strength [143]. Even though this method is suitable to obtain a more accurate and generalized learning model, it still has some limitations, which can reduce its reliability. One issue arises from research misconduct, wherein authors sometimes attempt to present materials as performing well, even though it does not align with the actual experimental results. Furthermore, in certain instances, research results are entirely fabricated or manipulated from the beginning, leading to fraudulent data. This can introduce inaccuracies and biases into the dataset, leading to unreliable models and misleading conclusions. Another issue is related to the uniformity of extracted information, where it would be hard to obtain data under the same processing conditions and microstructure evolution. For example, the super-hardness model was built basically on information related just to the composition of the materials, but other information, like the crystal structure, phases, grain structure, etc., was not included. Simply, this model cannot distinguish between polymorphous materials (diamond and graphite).

The initial dataset for a learning process can also be obtained from materials databases, in which the properties and structures of large number of materials are listed (hundreds of thousands). These databases serve as valuable resources for researchers, scientists, engineers, and other professionals working in the field of materials discovery and design. For this, there are several databases, such as Materials Project (MP), the Open Quantum Materials Database (OQMD), the Inorganic Crystal Structure Database (ICSD), and Automatic Flow for Materials Discovery (AFLOW). A simple comparison between these four databases is introduced in Figure 3, where MP and AFLOW incorporate high-throughput computational approaches and cover a broader range of materials, while ICSD deals with in inorganic crystal structures that were mostly reached using experimental techniques. OQMD, in turns, deals with the quantum mechanical properties of materials for energy applications. Hence, it is important to select a suitable database, and that is based on the specific requirements and the type of materials or properties that are of interest. One example for employing this type of data source is using the stability information of 25,880 compounds in MP to build a classification model that predicted stable perovskite structures [140]. The availability of such a substantial amount of data greatly expands the possibilities for materials discovery and design using learning techniques. However, it is important to have a proper understanding of the characteristics of the data, including the type of data and materials involved and approaches used to gather or to obtain these data. This understanding allows for the effective utilization and interpretation of the data, enabling researchers to make informed decisions and derive meaningful insights for materials science applications.

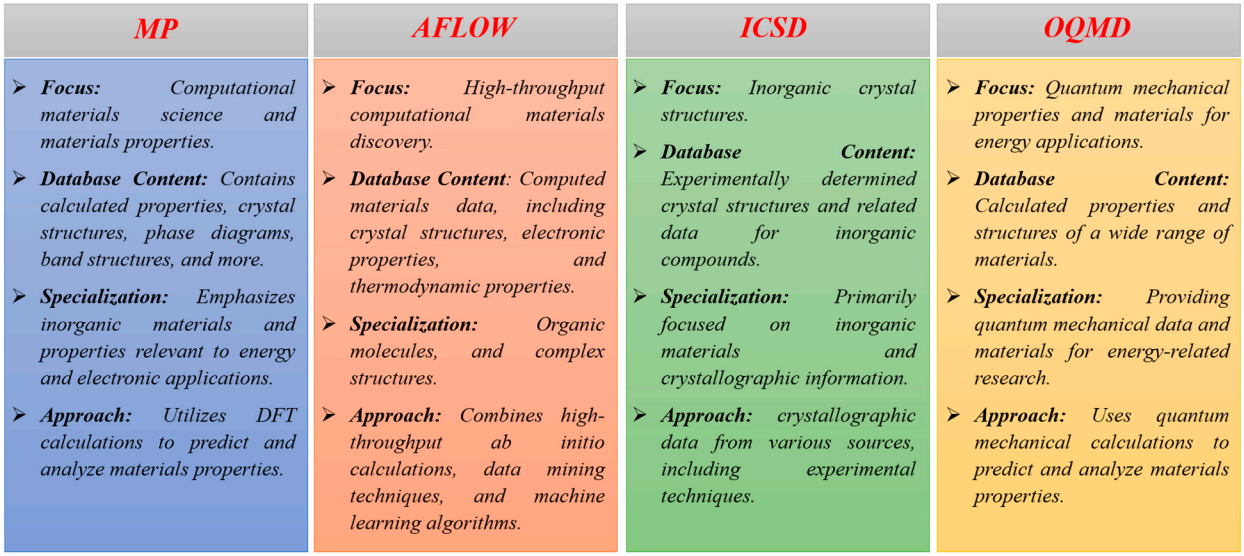

Figure 3. The main databases that are used in the field of material informatics and the differences between those in terms of focus, content, specialization and the approach of data collection.

3.2. Feature Generation and Engineering

Following initial data collection and processing, features that describe the materials in this dataset are usually generated and processed for further learning steps. The generation of material features involves extracting relevant information from the raw data to capture the key characteristics of the materials. These features can include physical properties such as density, melting point, or electrical conductivity as well as chemical properties like elemental composition, molecular structure, or bonding types. Additionally, features related to the fabrication process or specific applications of the materials may also be considered. Selecting the suitable set of features for a specific learning process is associated with various factors like the target of the learning process and the type of materials involved in the initial dataset. Here, three classes of materials features are mostly used in materials discovery and design aided by learning techniques. The first class is composition-related features, in which each material in the initial dataset is described through its composition and the properties of the elements that form the materials. These are usually physical, chemical, and electronic properties, such as the atomic number, atomic weight, electronegativity density, band gap, etc. For example, starting from the element properties listed in Jaafreh et al.'s work [140] (80 properties) and using two mathematical equations, like the average and maximum values, $2 \times 80 = 160$ distinct features can be generated to collectively describe a single material within the initial dataset. These features provide a comprehensive representation of the composition-related characteristics, allowing for a detailed understanding of the materials and facilitating further analysis and learning tasks. This type of feature has been widely employed in the design process of high-performance metallic alloys and amorphous materials [144]. In such cases, the focus is primarily on the composition-related features, and information regarding the crystal structure is typically not required. On the other hand, when dealing with various crystal systems, composition features become insufficient alone, and here the second class of features, which is related to the crystal structure, will be needed. In this type of feature, materials with same composition but different crystal structures, like diamond and graphite, can be distinguished from each other. For example, if the learning model is to predict the electrical conductivity, then using the composition features, both the diamond and graphite will be predicted to have the same conductivity, which technically is wrong, and here crystal features should be involved. By considering these features, the learning model can capture the distinct crystal

arrangements of diamond and graphite, allowing for accurate predictions that account for the varying electrical conductivities associated with their unique crystal structures. The third class of features is mainly needed when the raw data are extracted from experimental works, where the structure of materials is influenced by processing conditions. For this case, besides those obtained from the composition and crystal structure, features related to the processing parameters and evolved microstructures should be used in the learning process. For example, learning techniques were employed to design Al alloys with improved strength, where both the composition of Al alloy and age-hardening conditions (temperature and time) were included as features to build the learning model, by which high-strength Al alloys were reached [143].

3.3. Learning Algorithms and Error Metrics

After feature generation and processing, the final dataset that includes inputs (features) and the output (the parameter to be predicted) is involved in a training process through a suitable learning algorithm. This step is usually conducted based on a cross-validation (CV) process, which involves dividing the dataset into subsets or "folds" and iteratively training and testing the model on different combinations of these folds. By utilizing different subsets of the data, this process enhances the ability of the model to generalize over unseen data, which was excluded from the training data. In this step, selecting the learning technique is significant to reach models with high capability for solving the addressed problem. Generally, in materials science-related research, supervised learning algorithms are employed, where the input data are paired with corresponding output labels. These algorithms learn from the labeled examples to make predictions or classify new, unseen data. Here, various types of supervised learning algorithms are usually employed in materials science, which are summarized as follows:

- Linear Regression: Linear regression is a fundamental algorithm used for predicting continuous material properties based on input features. It models the relationship between the input variables and the target variable by fitting a linear equation. Linear regression is widely used in materials science for tasks such as predicting material strength, conductivity, or elasticity based on various input parameters.
- Support Vector Machine (SVM): SVM is a powerful algorithm used for both classification and regression tasks in materials science. In classification, SVM finds an optimal hyperplane that separates different classes of materials based on the input features. In regression, SVM can predict continuous material properties by finding a regression function that maximizes the margin between data points and the function. SVM has been used for tasks such as predicting the formability of perovskites and prediction of energy gaps in binary compounds [145].
- Decision Tree (DT): Decision trees are versatile algorithms that can be used for both classification and regression tasks. They partition the input feature space based on a series of binary decisions, creating a tree-like structure. Decision trees are interpretable and can handle both numerical and categorical features. They have been used in materials science for tasks such as the prediction of stability of multi-atoms structures, for instance [146].
- Random Forest (RF): Random forests are ensemble learning algorithms that combine multiple decision trees to make predictions. Each decision tree is trained on a random subset of the data, and the final prediction is obtained by averaging the predictions of individual trees. Random forests are robust, can handle high-dimensional data, and provide feature importance rankings. They have been used in materials science the prediction of the lattice thermal conductivity as an example [147].

- Gradient Boosting (GB): GB is another ensemble learning technique that combines multiple weak learners to create a strong predictive model. It iteratively builds decision trees, where each subsequent tree focuses on correcting the errors of the previous tree. Gradient boosting algorithms such as XGBoost and LightGBM have been applied in materials science for tasks like assessing the ductility and brittleness of magnesium alloys using elastic proxies [148].
- Neural Networks (NN): Neural networks, particularly deep neural networks, have gained significant popularity in materials science research. These algorithms consist of interconnected layers of nodes (neurons) that learn complex patterns from the input data. Neural networks can capture non-linear relationships and have been used for tasks such as image analysis, material property prediction, and molecular design.
- Gaussian Processes: Gaussian processes are probabilistic models that can be used for regression tasks in materials science. They model the uncertainty associated with predictions and provide a distribution over possible values for the target variable. Gaussian processes have been used for tasks such as representing atomic structures, symmetry adapted representations and more [149].

The choice of the suitable algorithm is controlled by several factors, like the size of the learning data, the type of the data, available computational resources and the desired accuracy and interpretability of the predictions. For example, in a small-sized dataset, deep neural networks algorithms are unsuitable, where such algorithms have many parameters, which enables them to learn intricate and non-linear patterns in the data. Accordingly, small datasets may not provide enough examples to capture the complexity of the underlying patterns. In addition, for image data, normal machine learning algorithms, like LR and SVM, are not suitable, especially when dealing with large and complex image datasets. It is often recommended to explore CNN-based architectures for image-related tasks, but SVMs can still be an alternative in certain scenarios or when computational resources are limited. In general, for a specific problem in material science to be handled through the learning process, the various types of algorithms are applied at once, and the selection of final model is made basically according to accuracy. Here, the learning model with the highest accuracy will be expected to perform the best in further steps. In this regard, several error metrics, also known as evaluation metrics or performance metrics, are usually used to determine the accuracy of models built based on the different types of learning algorithms. These metrics vary depending on the problem and data being analyzed. Commonly used error metrics include mean absolute error (MAE), mean squared error (MSE), root mean squared error (RMSE), R-squared (R^2), accuracy, precision, recall, F1-score, and confusion matrix. Each metric serves a specific purpose in evaluating different aspects of model performance. It is crucial to select the appropriate error metric that aligns with the objectives and characteristics of the problem at hand. For example, accuracy, precision, recall, F1-score, and confusion matrix are frequently used in binary classification problems, whereas MAE, MSE, RMSE, and R^2 are mostly used for regression-related problems.

3.4. Materials Design and Discovery

Reaching an accurate learning model that can catch the trend in a dataset is the final step in the learning process before moving to the application of this model in the targeted task. In materials science-related research, the target is always spinning around designing and discovering new materials that show high performance compared to the well-known counterparts. This can be conducted based on two different strategies. First is to start from already excited materials with relaxed structures, and those can be obtained from the materials databases. Starting from such materials, features are generated and are used as inputs in the learning model to predict the targeted property. For example, a learning

model built based on the lattice thermal conductivity of 110 crystalline materials was used to predict that conductivity of compounds presented in the ICSD database, where these compounds have now information related to the lattice thermal conductivity. Another way is to construct materials or compounds from scratch and then predict the required property based on the built learning model. Here, starting from well-known compounds and by chemical substitution in these compounds, a large number of compositions can be generated and then can be used as inputs in the model to predict the related property. For example, starting from $CaTiO_3$ and by the chemical substitution of Ca, Ti and O by other elements in a periodic table, 20 K compositions were constructed. The features generated for these compositions were provided to a learning model that was built to predict the elastic moduli of crystalline materials, and thus, the elastic moduli of new materials are obtained and can be handled for further experimentation as needed.

4. Current Research on Electrolytic Materials Designed by ML

AI techniques were used to discover new electronic materials with improved performance as compared to traditional materials employed in this application. Here, the discovery process is usually considered based on various parameters, including ionic conductivity, electrical conductivity, mechanical stability, thermometrical stability, and electrochemical stability. For example, as a solid-state electrolyte (SSE), materials with high ionic conductivity and improved electrochemical stability are needed to optimize the performance of the solid-state LIBs.

Choi et al. [84] used ML to search for SSEs with improved mechanical performance, and this was conducted based on the elastic moduli of the candidate materials (Figure 4). For securing a stable interface between Li metal and the electrolyte, and to suppress dendrite generation and growth, the candidate materials should have a high shear modulus, which is twice as large as that of Li metals (8.5 GPa). The learning data used in this work were obtained from MP, where the elastic moduli (shear (G) and bulk (K)) calculated by DFT of 15,986 compounds listed in MP were extracted, and the composition features of these compounds were generated. The predictive model was built using the LightGBM algorithm with R^2 values of 0.819 and 0.863 for G and K, respectively, and this model was then employed in a prediction process to find the moduli of 2845 stable Li compounds that have no active elements (K, Na, and Ca). The results showed that the oxide-based electrolytes showed superior mechanical properties for this application. Similar work was reported by Satpati et al. [77], who examined the capabilities of various ML algorithms to build an accurate model: those were DT, RF and GB.

The mechanical moduli were also used by Ahmed at al. [76]. to assist the evaluation of interfacial stability between Li and electrolyte materials, and this was basically conducted using a deep learning technique(Figure 5). In their work, a learning model was built based on moduli data involving the G and elastic constant (C_{11}, C_{12}, and C_{44}) of crystalline materials obtained from Materials Projects. For building the model, the structures of the materials in the initial dataset alongside the outputs (G, C_{11}, C_{12}, and C_{44}) were involved in a learning process using a graph convolutional neural network (GCNN). Based on this technique, the features of the materials included in the initial dataset are extracted and learned by the neural network to build the model.

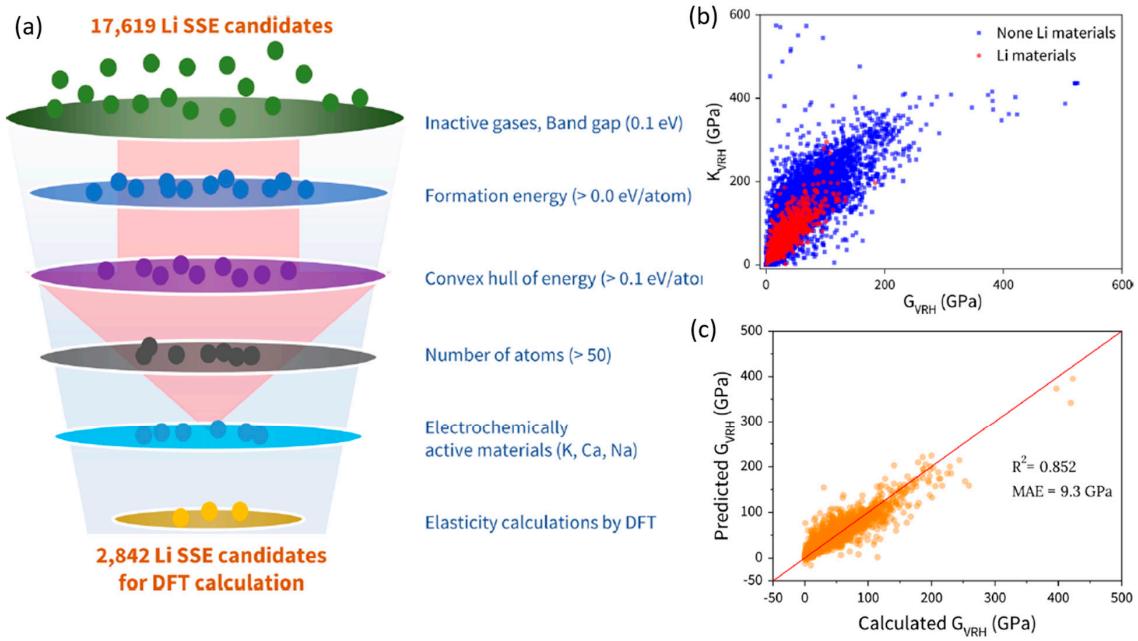

Figure 4. An overview of the work of Choi et al. [84] which illustrates the process of discovery of mechanically superior Li-ion solid-state electrolytes. (**a**) The screening process for the collection of potential solid-state Li-ion materials. (**b**) Correlation of the shear vs. bulk modulus (K_{VRH} vs. B_{VRH}) of the training database. (**c**) The ML predicted vs. DFT calculated shear modulus along with common error metrics (R^2 and MAE). Adapted with permission from Ref. [84].

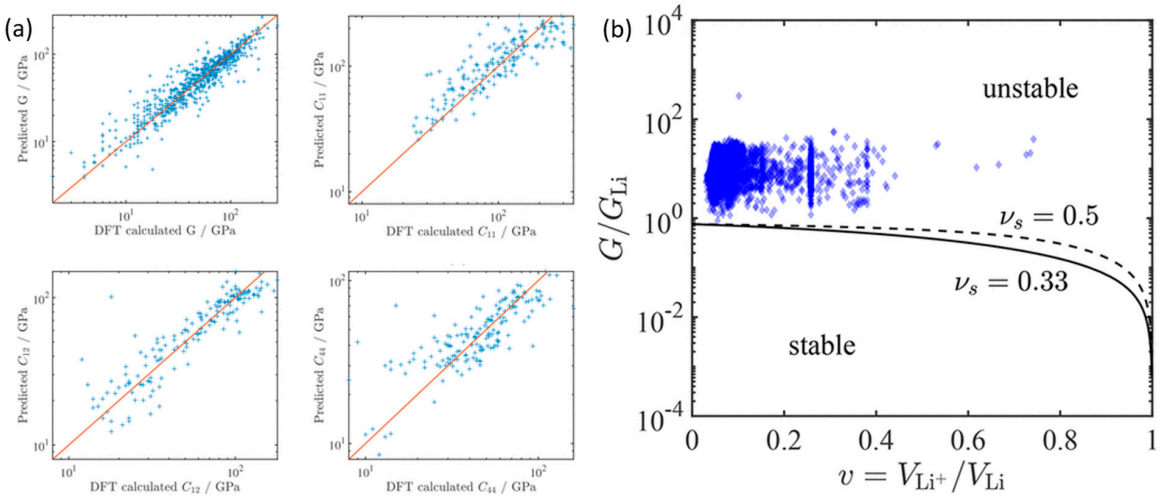

Figure 5. Overview of the work of Ahmad et al. [76] depicting the computational screening of inorganic solid electrolytes for dendrite suppression in lithium metal anodes using machine learning. (**a**) Plots comparing machine-predicted elastic properties (shear modulus G and elastic constants C11, C12, C44) to DFT-calculated values. CGCNN predicts shear modulus, while gradient boosting and kernel ridge regression predict elastic constants. (**b**) Isotropic stability diagram depicts the position of screened solid electrolytes with GLi as the shear modulus of Li (3.4 GPa). The critical G/GLi line, crucial for stability assessment, is weakly dependent on Poisson's ratio; lines for νs = 0.33 and 0.5 serve as reliable stability indicators. Darker regions signify a higher number of materials in that region. Adapted with permission from Ref. [76].

Another work by Zhao et al. [75] reported the application of ML to assist the design experiments of lithium aluminum titanium phosphate (LATP) as a solid electrolyte in LIBs, where LATP was selected due to its high ionic conductivity (Figure 6). In this work, the synthesis conditions of LATP were adjusted through a Gaussian process (GP)-based

Bayesian optimization, where the conditions needed to prepare a highly pure material with a maximum ionic conductivity (10^{-3} S/cm) were found. Here, three experimental parameters including the concentration of precursors, sintering temperature, and sintering time were used as inputs, whereas density and ionic conductivity were the output. The model built based on 80 experiments under the various conditions of concentration, temperature, and time was used to find the conditions for reaching the material with high purity and improved ionic conductivity. Recently, ML was used to find the features that highly influence the mobility of cations within crystalline materials to design a solid electrolyte with high ionic conductivity. For training the ML model, data containing energy barriers of ion migration obtained based on DFT calculations were collected [78]. The results showed that the migration pass distance and width and anion polarizability significantly influence the energy barriers of cation migration.

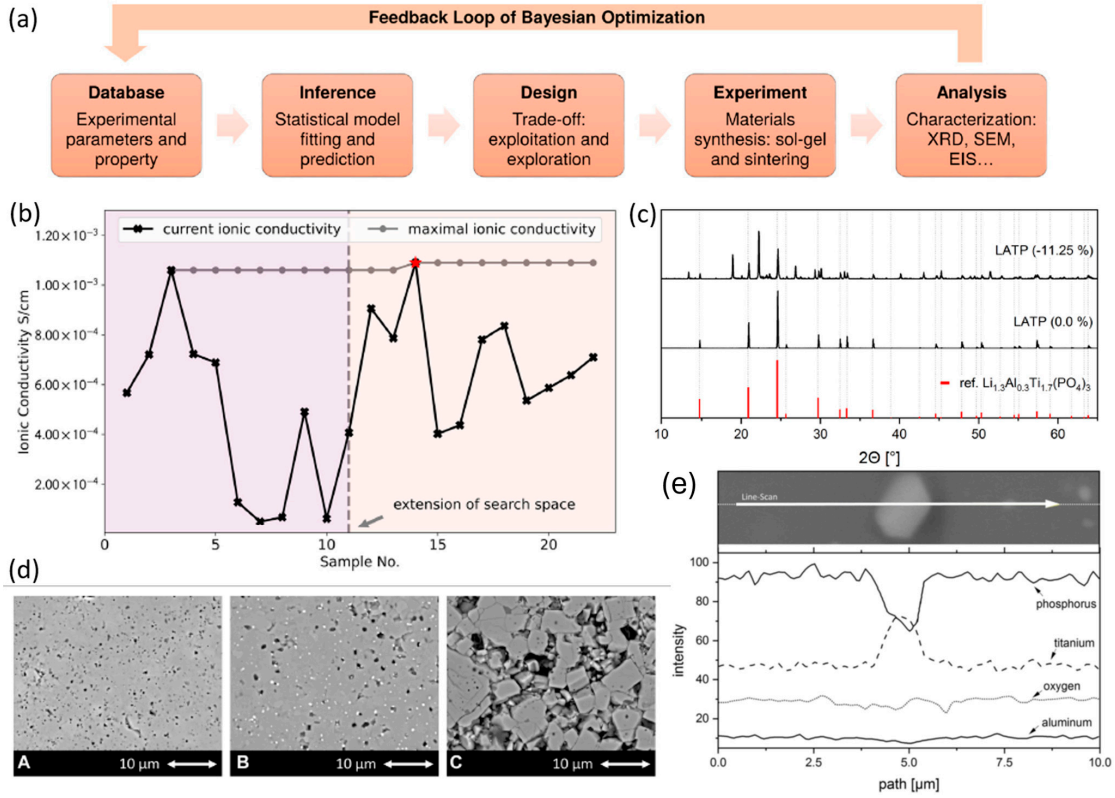

Figure 6. An overview of Zhao et al.'s work [75] regarding the experiments design of solid-state lithium aluminum titanium phosphate electrolyte using machine learning. (**a**) The Bayesian optimization workflow involves five key steps: (1) collecting initial experimental data for machine learning model training; (2) fitting an inference model, like Gaussian process regression; (3) predicting the property in the search space, considering both prediction and uncertainty for optimal experimental configuration; (4) conducting the experiment to synthesize a new sample; and (5) validating the new sample's performance with results feeding back into the initial dataset for subsequent iterations. (**b**) Ionic conductivity values (black line) fluctuate over four iterations, reflecting exploration–exploitation dynamics, showing an overall upward trend. The model identifies peak conductivity values (red star) within iterations. (**c**) X-ray diffraction patterns: LATP (−11.25 wt%) sintered at 1000 °C for 450 min, LATP (0.0 wt%) sintered at 900 °C for 30 min, and reference $Li_{1.3}Al_{0.3}Ti_{1.7}(PO_4)_3$ pattern (in red). (**d**) Microstructure: (A) LATP (0.0 wt%) sintered at 900 °C for 30 min; (B) LATP (−11.25 wt%) sintered at 1000 °C for 450 min; (C) LATP (0.0 wt%) sintered at 1000 °C for 450 min. (**e**) EDX-line-scan: bright second phase particle in sintered LATP (−11.25 wt%) sample, with a noticeable titanium intensity increase at the bright region, strongly suggesting the second phase is likely TiO_2. Adapted with permission from Ref. [75].

Recently, an ML model has been built based on data collected from other works reported on the preparation and characterization of solid electrolytes for LIBs [147] (Figures 7 and 8). This work was mainly focused on ceramic based electrolytes, and to calculate the activation energy, working temperature was also used in the model as a feature alongside the composition features. The model was successfully built using an RF algorithm, and this model was used to find solid electrolytes that are expected to show high ionic conductivity at room temperature. Indeed, screening 30,000 compositions presented in the ICSD database reached 67 Li-S based compounds with high ionic conductivity (>0.01 S/cm) at room temperature. In addition, the ionic conductivity and thermomechanical stability of solid electrolytes in LIBs were also optimized using ML techniques [148]. In addition to the ionic conductivity, the thermomechanical stability of solid electrolytes in LIBs was also targeted in ML works. One work reported recently by the present group investigated the applicability of ML techniques to optimize the thermal stability of Li solid-state electrolytes [148]. The learning data used in the work contained the thermal expansion coefficient value of solid materials (5578) presented in AFLOW. The composition and crystal structure of these materials were used to generate a set of 272 features for one material. To assess the performance of various algorithms, extra tree (XT), random forest (RF), extreme gradient boost (XGB), and gradient boosting (GB) were optimized for prediction and compared. The XT-based model showed the best performance compared to other models. Further validations were presented using the calculations of the electron localization function (ELF) based on DFT. The ELF results obtained for $MgBe_{13}$ and $MgPd_2$ were consistent with the predictions made based on the XT-based model built in this study. The built model was then used to predict electrolyte–cathode pairs that are highly thermomechanically compatible.

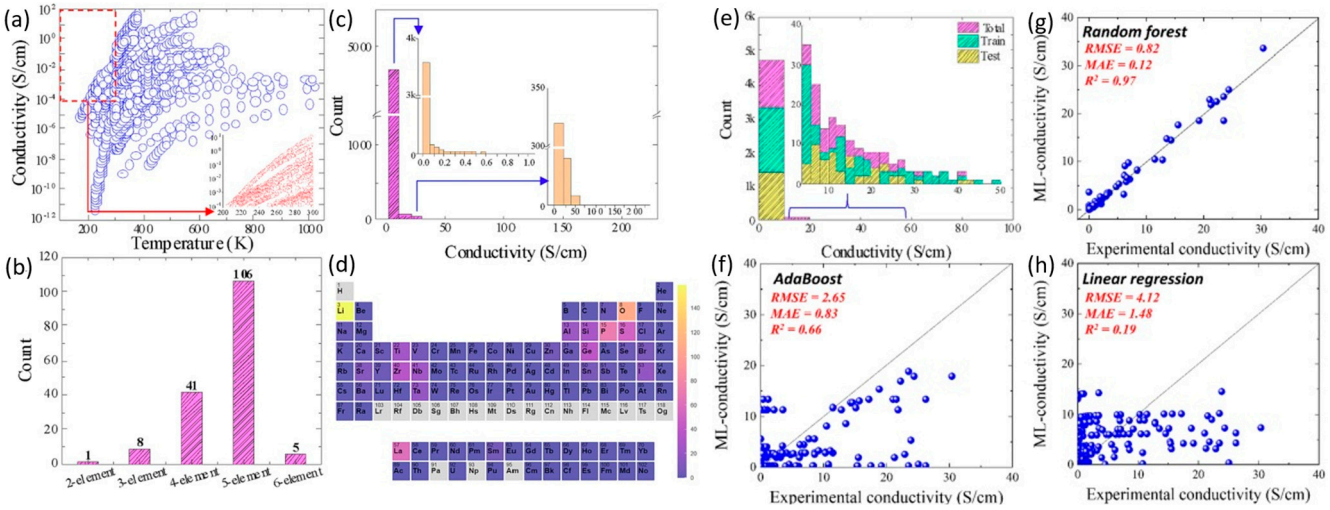

Figure 7. An overview of Pereznieto et al.'s work [147] describing the employment of ML modeling in the prediction of Li-ion based electrolytes ionic conductivity with temperature. (**a**) Scatter plot describing the characteristics of the initial dataset that have been collected for the work. (**b**) Number of elements of each compound in the initial dataset. (**c**) A histogram of the collected ionic conductivity of the initial dataset. (**d**) The element distribution heatmap of the compounds that have been collected for the initial dataset. (**e**) The representative split histogram that is used for the ML modeling process. (**f**–**h**) Scatter plot accompanied by the R^2 for the ML algorithms used in Pereznieto et al.'s work [147] for Adaboost, random forest and linear regression algorithms, respectively. Adapted with permission from Ref. [147].

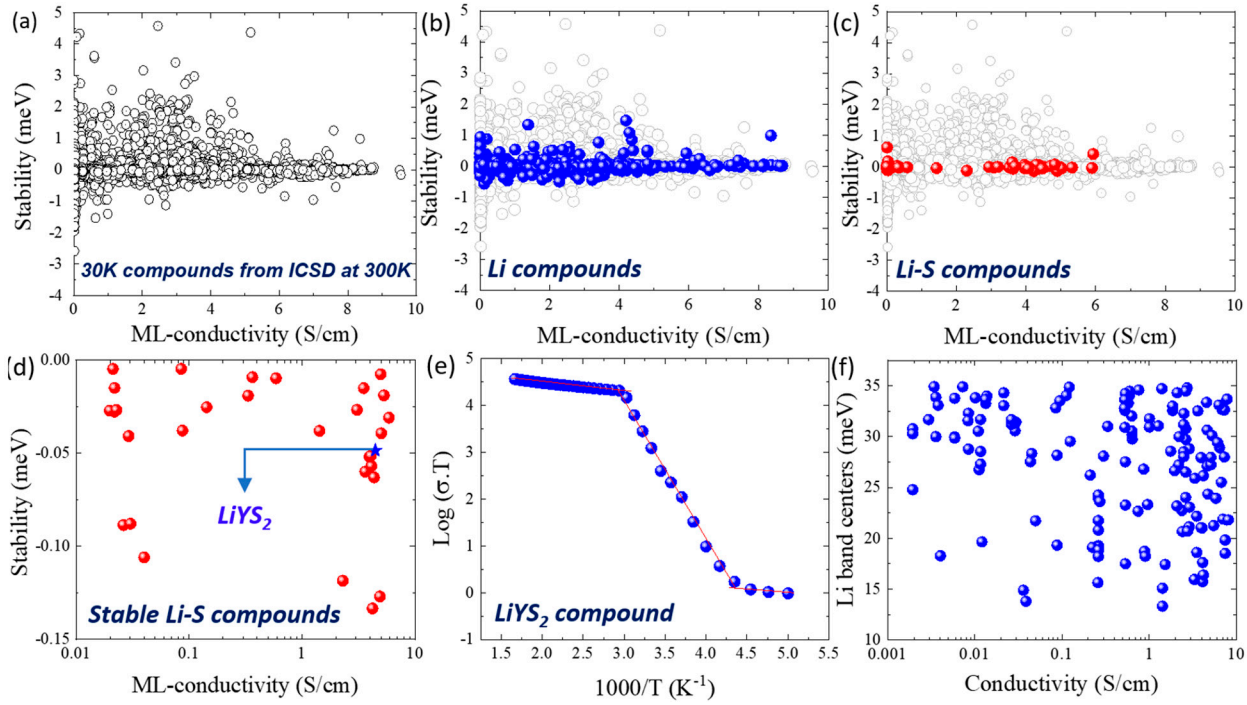

Figure 8. An overview of Pereznieto et al.'s work [147] describing the employment of ML modeling in the prediction of Li-ion based electrolytes ionic conductivity with temperature. (**a**) The ML prediction of the ionic conductivity for 30 K materials included in the ICSD database at 300 K. (**b**,**c**) Highlight of Li and Li-S compounds in the initial 30 K Li-based electrolytes displayed in (**a**). (**d**) A detailed figure of the stable Li-S compounds ($E_h < 0$) that show considerable ionic conductivity. (**e**) The ionic conductivity vs. temperature behavior of LiY_2 as a potential viable Li-ion based electrolyte. (**f**) The relationship between the band centers first. Adapted with permission from Ref. [148].

Not just solid electrolytes but also liquid ones were targeted in machine learning works to optimize their performance in LIBs. A work reported by Duong et al. [79] utilized machine learning to find a suitable combination of additives to be included with $LiPF_6$, which is a well-known liquid electrolyte in LIBs. For this purpose, various additive materials including ethylene carbonate (EC), ethyl methyl carbonate (EMC), lithium bis(oxalate) borate (LiBOB), vinylene carbonate (VC), and fluoroethylene carbonate (FEC) were used in different ratios with the base electrolyte ($LiPF_6$). In addition, two other features were included as input: the ratio of negative and positive electrodes (N/P ratio) and the number of cycles. As an output, capacities of assembled cells were determined through electrochemical tests. An artificial neural network (ANN) technique was used to train the model that could relate between the additives type and amounts with the performance of the cell (capacity). The prediction results reached based on the built ANN model showed that the optimum composition to achieve high capacity was 1.1 M $LiPF_6$ in FEC: EC: EMC (0.7: 2.8: 6.5) (%v) with a combination of 0.6 %wt. LiBOB and 0.01 %wt. VC. In addition to the composition of the liquid electrolytes used in LIBs, ML techniques were employed to determine the concentration of electrolytes during charging and discharging processes. This was reported by Ellis et al. [65] who built a learning model by which the concentration of $LiPF_6$ in an organic solvent of EC and dimethyl carbonate (DMC) are determined through the Fourier transform infrared (FTIR) spectrum of the electrolyte (Figure 9). Initially, the FTIR spectra of $LiPF_6$-based electrolyte with various compositions were recorded, and then features were extracted from the spectra. The model was trained using the extracted features (input) and the concentration of the related electrolyte (output), and this was conducted using a linear algorithm. The learning process resulted in a simple predictive

model that could relate the concentration of the electrolyte, in terms of $LiPF_6$ concentration and the volume % ratio of EC in the EC/DMC, and the FTIR-based features.

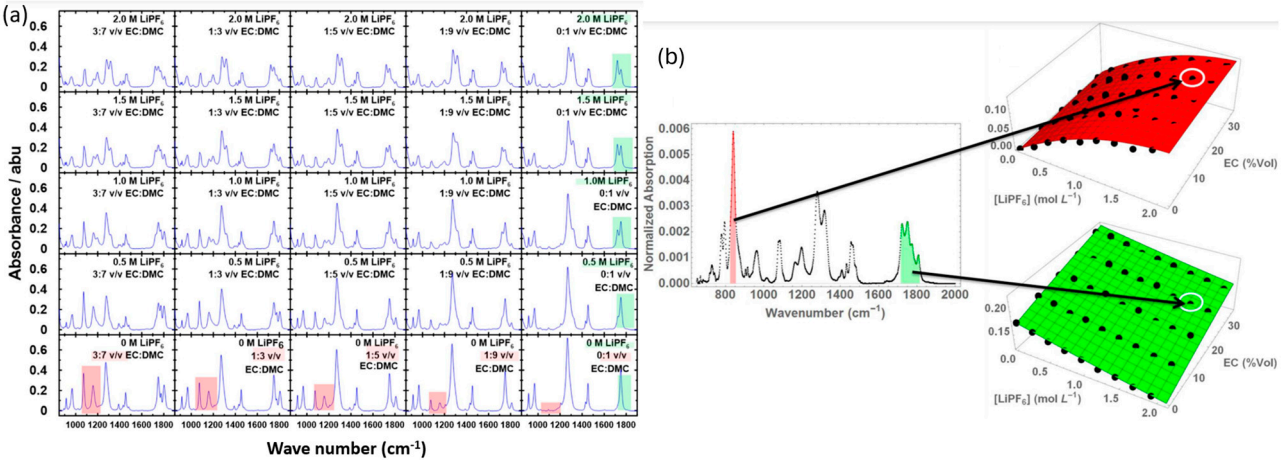

Figure 9. An overview of the work of Ellis et al. [65] in regard to implementing machine learning techniques in determining the electrolyte components concentration determination. (**a**) Evolution of ATR-FTIR spectra in electrolyte solutions featuring varying concentrations of LiPF6, EC, and DMC. Green highlights signify the progression of a spectral feature strongly linked to (LiPF6) in DMC solutions, while red highlights denote the evolution of a spectral feature correlated with (EC) in DMC solutions. (**b**) FTIR spectrum depicting an electrolyte solution with 1.75 M LiPF6 and 25% (v) EC in DMC. Red highlights a distinct spectral feature strongly associated with (LiPF6), while green highlights a notable spectral feature correlated with (EC). The variation in these features is illustrated across a spectrum of electrolyte compositions. Adapted with permission from Ref. [65].

In the above discussed works, the data used in the learning process were obtained from two different sources. The first is Materials Projects, where the moduli of a large number of materials were extracted and included in the learning process [75,76]. The second was fresh experiments to determine the needed parameter for the learning process, like measuring the capacity of various cells constructed using electrolytes with a range of compositions [65]. In general, the second source is somehow controllable and can be directed according to the target of the learning process. For example, if the ionic conductivity is to be optimized through the learning process, then ionic conductivity is measured under various conditions, like the composition of the electrolyte, and the ionic conductivities and related conditions are included the learning process to find the best conditions that lead to high ionic conductivity. On the other hand, for building an accurate ML model using this source, a large number of data are needed, and this, in turn, can be limited due to the high cost of such a path. Here, data from other works can be included to enhance the quality of the model, but this is also constrained by the human capability to deal with a huge number of works in terms of "*text mining*" (collecting related papers, the classification of these papers, and the final extraction of the useful knowledge, which can be included in further learning processes). For this purpose, machine-based text mining techniques are employed in order to obtain domain knowledge by which machines can deeply learn compared to data processed using human-based text mining. Two works by Olivetti et al. [149,150] were reported on the applicability of text mining in the field of LIBs materials. The first work was mainly focused on the electrode's materials [149], whereas solid electrolytes were reported in the second work [150]. In these works, ~1000 articles that reported on the preparation, characterization, and performance of solid electrolytes were involved in a text mining process to extract the knowledge, which was analyzed to obtain some insights on the relationship between the composition, processing conditions, and performance of solid electrolytes, but no machine learning process was conducted.

This study mainly handles the work reported on the preparation and performance of some well-known electrolytes including Li_2S-P_2S_5, $Li_7P_3S_{11}$, β-Li_3PS_4, LGPS and garnet LLZO oxides, which were found to have high conductivities at RT (>10^{-4} S/cm), and here processing temperatures (drying, annealing, calcination and sintering) were analyzed. The extracted data showed that the densification temperatures of Li garnet ceramics are higher than those of other electrolytes. In addition, it was found that Li garnet ceramics are most sintered at temperatures higher than those used for drying, annealing, and calcination. Since the ML process was missing from this work, further efforts can be made to employ the mined data in a learning process that can be used to optimize the processing conditions of these types of solid electrolytes.

5. Conclusions

In conclusion, this review highlights the research gap in the application of learning techniques to the design of high-performance electrolytic materials for Li-ion batteries (LIBs), emphasizing the potential of AI-driven methods to accelerate both fundamental and applied research in materials science. By using these techniques, significant progress has already been made in discovering new compositions and processing conditions for electrolytic materials that exhibit the desirable performance in LIBs. Despite these advancements, challenges remain, particularly the lack of usable data to build accurate predictive models. This underscores the need for further development in data collection and processing methods. One promising solution is automated text mining, which can efficiently extract valuable insights from vast amounts of unstructured scientific literature, addressing the data limitations and uncovering hidden patterns in materials discovery. The integration of text mining not only holds promise for improving predictive models but also offers a broader impact by enabling a more efficient exploration of scientific knowledge across various fields. These advancements signal a transformative shift in how materials science and engineering research will evolve in the future.

Author Contributions: H.A. designed the idea and collected the required references, H.A. and R.J. writing—original draft preparation, H.A., K.H. and J.-G.K. revised the first draft, K.H. and J.-G.K. supervision, all authors contributed to the discussion of main concepts. All authors have read and agreed to the published version of the manuscript.

Funding: This research received no external funding.

Data Availability Statement: No new data were created or analyzed in this study.

Conflicts of Interest: The authors declare no conflict of interest.

References

1. Yan, Q.; Yu, J.; Suram, S.K.; Zhou, L.; Shinde, A.; Newhouse, P.F.; Chen, W.; Li, G.; Persson, K.A.; Gregoire, J.M.; et al. Solar fuels photoanode materials discovery by integrating high-throughput theory and experiment. *Proc. Natl. Acad. Sci. USA* **2017**, *114*, 3040–3043. [CrossRef] [PubMed]
2. Na, G.S.; Chang, H. A public database of thermoelectric materials and system-identified material representation for data-driven discovery. *NPJ Comput. Mater.* **2022**, *8*, 214. [CrossRef]
3. Oliveira, G.D.S.; Candido, I.C.M.; Lima, R.M.A.P.; De Oliveira, H.P. All-In-One Energy Harvesting/Storage Integrated Systems Based on Eggshell Membranes. *ACS Appl. Electron. Mater.* **2022**, *4*, 4708–4718. [CrossRef]
4. Saal, J.E.; Kirklin, S.; Aykol, M.; Meredig, B.; Wolverton, C. Materials Design and Discovery with High-Throughput Density Functional Theory: The Open Quantum Materials Database (OQMD). *JOM* **2013**, *65*, 1501–1509. [CrossRef]
5. Schmidt, J.; Marques, M.R.G.; Botti, S.; Marques, M.A.L. Recent advances and applications of machine learning in solid-state materials science. *NPJ Comput. Mater.* **2019**, *5*, 83. [CrossRef]
6. Kim, C.; Pilania, G.; Ramprasad, R. Machine Learning Assisted Predictions of Intrinsic Dielectric Breakdown Strength of ABX_3 Perovskites. *J. Phys. Chem. C* **2016**, *120*, 14575–14580. [CrossRef]

7. Faber, F.A.; Lindmaa, A.; Von Lilienfeld, O.A.; Armiento, R. Machine Learning Energies of 2 Million Elpasolite (ABC_2D_6) Crystals. *Phys. Rev. Lett.* **2016**, *117*, 135502. [CrossRef]
8. Zheng, X.; Zheng, P.; Zhang, R.-Z. Machine learning material properties from the periodic table using convolutional neural networks. *Chem. Sci.* **2018**, *9*, 8426–8432. [CrossRef]
9. Chakraborty, P.; Liu, Y.; Ma, T.; Guo, X.; Cao, L.; Hu, R.; Wang, Y. Quenching Thermal Transport in Aperiodic Superlattices: A Molecular Dynamics and Machine Learning Study. *ACS Appl. Mater. Interfaces* **2020**, *12*, 8795–8804. [CrossRef]
10. Qian, X.; Yang, R. Machine learning for predicting thermal transport properties of solids. *Mater. Sci. Eng. R. Rep.* **2021**, *146*, 100642. [CrossRef]
11. Wei, H.; Bao, H.; Ruan, X. Genetic algorithm-driven discovery of unexpected thermal conductivity enhancement by disorder. *Nano Energy* **2020**, *71*, 104619. [CrossRef]
12. Li, M.; Lu, J.; Chen, Z.; Amine, K. 30 Years of Lithium-Ion Batteries. *Adv. Mater.* **2018**, *30*, 1800561. [CrossRef]
13. Mueller, T.; Hautier, G.; Jain, A.; Ceder, G. Evaluation of Tavorite-Structured Cathode Materials for Lithium-Ion Batteries Using High-Throughput Computing. *Chem. Mater.* **2011**, *23*, 3854–3862. [CrossRef]
14. Nitta, N.; Wu, F.; Lee, J.T.; Yushin, G. Li-ion battery materials: Present and future. *Mater. Today* **2015**, *18*, 252–264. [CrossRef]
15. Li, C.; Poplawsky, J.; Wu, Y.; Lupini, A.R.; Mouti, A.; Leonard, D.N.; Paudel, N.; Jones, K.; Yin, W.; Al-Jassim, M.; et al. From atomic structure to photovoltaic properties in CdTe solar cells. *Ultramicroscopy* **2013**, *134*, 113–125. [CrossRef]
16. Li, T.; Chen, Z.X.; Cao, Y.L.; Ai, X.P.; Yang, H.X. Transition-metal chlorides as conversion cathode materials for Li-ion batteries. *Electrochim. Acta* **2012**, *68*, 202–205. [CrossRef]
17. Vengatesan, S.; Jayakumar, A.; Sadasivuni, K.K. FCEV vs. BEV—A short overview on identifying the key contributors to affordable & clean energy (SDG-7). *Energy Strategy Rev.* **2024**, *53*, 101380. [CrossRef]
18. Goodenough, J.B.; Park, K.-S. The Li-Ion Rechargeable Battery: A Perspective. *J. Am. Chem. Soc.* **2013**, *135*, 1167–1176. [CrossRef] [PubMed]
19. Tian, Y.; Zeng, G.; Rutt, A.; Shi, T.; Kim, H.; Wang, J.; Koettgen, J.; Sun, Y.; Ouyang, B.; Chen, T.; et al. Promises and Challenges of Next-Generation "Beyond Li-ion" Batteries for Electric Vehicles and Grid Decarbonization. *Chem. Rev.* **2021**, *121*, 1623–1669. [CrossRef]
20. Lewis, G.N.; Keyes, F.G. The potential of the lithium electrode. *J. Am. Chem. Soc.* **1913**, *35*, 340–344. [CrossRef]
21. Selim, R.G.; Hill, K.; Rao, M. *Research and Development of a High Capacity, Nonaqueous Secondary Battery*; PR Mallory & Company: Springfield, VA, USA, 1966.
22. Nzereogu, P.U.; Omah, A.D.; Ezema, F.I.; Iwuoha, E.I.; Nwanya, A.C. Anode materials for lithium-ion batteries: A review. *Appl. Surf. Sci. Adv.* **2022**, *9*, 100233. [CrossRef]
23. Lee, M.J.; Han, J.; Lee, K.; Lee, Y.J.; Kim, B.G.; Jung, K.-N.; Kim, B.J.; Lee, S.W. Elastomeric electrolytes for high-energy solid-state lithium batteries. *Nature* **2022**, *601*, 217–222. [CrossRef]
24. Barbosa, J.C.; Gonçalves, R.; Costa, C.M.; Lanceros-Méndez, S. Toward Sustainable Solid Polymer Electrolytes for Lithium-Ion Batteries. *ACS Omega* **2022**, *7*, 14457–14464. [CrossRef]
25. Cai, J.; Wang, Z.; Wu, S.; Han, Y.; Li, J. A Machine Learning Shortcut for Screening the Spinel Structures of Mg/Zn Ion Battery Cathodes with a High Conductivity and Rapid Ion Kinetics. *Energy Storage Mater.* **2021**, *42*, 277–285. [CrossRef]
26. Chi, P.-W.; Paul, T.; Su, Y.-H.; Su, K.-H.; Su, C.-Y.; Wu, P.M.; Wang, S.-F.; Wu, M.-K. A study on Ti-doped Fe3O4 anode for Li ion battery using machine learning, electrochemical and distribution function of relaxation times (DFRTs) analyses. *Sci. Rep.* **2022**, *12*, 4851. [CrossRef]
27. Louis, S.-Y.; Siriwardane, E.M.D.; Joshi, R.P.; Omee, S.S.; Kumar, N.; Hu, J. Accurate Prediction of Voltage of Battery Electrode Materials Using Attention-Based Graph Neural Networks. *ACS Appl. Mater. Interfaces* **2022**, *14*, 26587–26594. [CrossRef]
28. Xu, H.; Zhu, J.; Finegan, D.P.; Zhao, H.; Lu, X.; Li, W.; Hoffman, N.; Bertei, A.; Shearing, P.; Bazant, M.Z. Guiding the Design of Heterogeneous Electrode Microstructures for Li-Ion Batteries: Microscopic Imaging, Predictive Modeling, and Machine Learnings. *Adv. Energy Mater.* **2021**, *11*, 2003908. [CrossRef]
29. Ha, M.; Hajibabaei, A.; Kim, D.Y.; Singh, A.N.; Yun, J.; Myung, C.W.; Kim, K.S. Al-Doping Driven Suppression of Capacity and Voltage Fadings in 4d-Element Containing Li-Ion-Battery Cathode Materials: Machine Learning and Density Functional Theory. *Adv. Energy Mater.* **2022**, *12*, 2201497. [CrossRef]
30. Wu, W.; Wang, S.; Sun, Q. Topological Quantum Cathode Materials for Fast Charging Li-Ion Battery Identified. *Adv. Theory Simul.* **2022**, *5*, 2100350. [CrossRef]
31. Allam, O.; Cho, B.W.; Kim, K.C.; Jang, S.S. Application of DFT-based machine learning for developing molecular electrode materials in Li-ion batteries. *RSC Adv.* **2018**, *8*, 39414–39420. [CrossRef]
32. Attarian Shandiz, M.; Gauvin, R. Application of machine learning methods for the prediction of crystal system of cathode materials in lithium-ion batteries. *Comput. Mater. Sci.* **2016**, *117*, 270–278. [CrossRef]
33. Houchins, G.; Viswanathan, V. An accurate machine-learning calculator for optimization of Li-ion battery cathodes. *J. Chem. Phys.* **2020**, *153*, 054124. [CrossRef] [PubMed]

34. Carvalho, R.P.; Marchiori, C.F.N.; Brandell, D.; Araujo, C.M. Artificial intelligence driven in-silico discovery of novel organic lithium-ion battery cathodes. *Energy Storage Mater.* **2022**, *44*, 313–325. [CrossRef]
35. Bölle, F.T.; Bhowmik, A.; Vegge, T.; Maria García Lastra, J.; Castelli, I.E. Automatic Migration Path Exploration for Multivalent Battery Cathodes using Geometrical Descriptors. *Batter Supercaps* **2021**, *4*, 1516–1524. [CrossRef]
36. Manna, S.; Roy, D.; Das, S.; Pathak, B. Capacity prediction of K-ion batteries: A machine learning based approach for high throughput screening of electrode materials. *Mater. Adv.* **2022**, *3*, 7833–7845. [CrossRef]
37. Xue, Z.; Li, J.; Pianetta, P.; Liu, Y. Data-Driven Lithium-Ion Battery Cathode Research with State-of-the-Art Synchrotron X-ray Techniques. *Acc. Mater. Res.* **2022**, *3*, 854–865. [CrossRef]
38. Gao, X.; Liu, X.; He, R.; Wang, M.; Xie, W.; Brandon, N.P.; Wu, B.; Ling, H.; Yang, S. Designed high-performance lithium-ion battery electrodes using a novel hybrid model-data driven approach. *Energy Storage Mater.* **2021**, *36*, 435–458. [CrossRef]
39. Honrao, S.J.; Yang, X.; Radhakrishnan, B.; Kuwata, S.; Komatsu, H.; Ohma, A.; Sierhuis, M.; Lawson, J.W. Discovery of novel Li SSE and anode coatings using interpretable machine learning and high-throughput multi-property screening. *Sci. Rep.* **2021**, *11*, 16484. [CrossRef] [PubMed]
40. Ko, S.; Obukata, T.; Shimada, T.; Takenaka, N.; Nakayama, M.; Yamada, A.; Yamada, Y. Electrode potential influences the reversibility of lithium-metal anodes. *Nat. Energy* **2022**, *7*, 1217–1224. [CrossRef]
41. Huang, J.-X.; Csányi, G.; Zhao, J.-B.; Cheng, J.; Deringer, V.L. First-principles study of alkali-metal intercalation in disordered carbon anode materials. *J. Mater. Chem. A* **2019**, *7*, 19070–19080. [CrossRef]
42. Kabiraj, A.; Mahapatra, S. High-throughput assessment of two-dimensional electrode materials for energy storage devices. *Cell Rep. Phys. Sci.* **2022**, *3*, 100718. [CrossRef]
43. Guo, X.; Chen, C.; Ong, S.P. Intercalation Chemistry of the Disordered Rocksalt $Li_3V_2O_5$ Anode from Cluster Expansions and Machine Learning Interatomic Potentials. *Chem. Mater.* **2023**, *35*, 1537–1546. [CrossRef]
44. Zhang, X.; Zhou, J.; Lu, J.; Shen, L. Interpretable learning of voltage for electrode design of multivalent metal-ion batteries. *NPJ Comput. Mater.* **2022**, *8*, 175. [CrossRef]
45. Eremin, R.A.; Zolotarev, P.N.; Ivanshina, O.Y.; Bobrikov, I.A. Li(Ni,Co,Al)O_2 Cathode Delithiation: A Combination of Topological Analysis, Density Functional Theory, Neutron Diffraction, and Machine Learning Techniques. *J. Phys. Chem. C* **2017**, *121*, 28293–28305. [CrossRef]
46. Wang, C.; Aoyagi, K.; Wisesa, P.; Mueller, T. Lithium Ion Conduction in Cathode Coating Materials from On-the-Fly Machine Learning. *Chem. Mater.* **2020**, *32*, 3741–3752. [CrossRef]
47. Niri, M.F.; Liu, K.; Apachitei, G.; Ramirez, L.R.; Lain, M.; Widanage, D.; Marco, J. Machine learning for optimised and clean Li-ion battery manufacturing: Revealing the dependency between electrode and cell characteristics. *J. Clean. Prod.* **2021**, *324*, 129272. [CrossRef]
48. Moses, I.A.; Joshi, R.P.; Ozdemir, B.; Kumar, N.; Eickholt, J.; Barone, V. Machine Learning Screening of Metal-Ion Battery Electrode Materials. *ACS Appl. Mater. Interfaces* **2021**, *13*, 53355–53362. [CrossRef] [PubMed]
49. Joshi, R.P.; Eickholt, J.; Li, L.; Fornari, M.; Barone, V.; Peralta, J.E. Machine Learning the Voltage of Electrode Materials in Metal-Ion Batteries. *ACS Appl. Mater. Interfaces* **2019**, *11*, 18494–18503. [CrossRef]
50. Tsuchimoto, A.; Okubo, M.; Yamada, A. Machine Learning-based Comprehensive Survey on Lithium-rich Cathode Materials. *Electrochemistry* **2023**, *91*, 037007. [CrossRef]
51. Wang, G.; Fearn, T.; Wang, T.; Choy, K.-L. Machine-Learning Approach for Predicting the Discharging Capacities of Doped Lithium Nickel–Cobalt–Manganese Cathode Materials in Li-Ion Batteries. *ACS Cent. Sci.* **2021**, *7*, 1551–1560. [CrossRef]
52. Finegan, D.P.; Squires, I.; Dahari, A.; Kench, S.; Jungjohann, K.L.; Cooper, S.J. Machine-Learning-Driven Advanced Characterization of Battery Electrodes. *ACS Energy Lett.* **2022**, *7*, 4368–4378. [CrossRef]
53. Kim, M.; Kang, S.; Gyu Park, H.; Park, K.; Min, K. Maximizing the energy density and stability of Ni-rich layered cathode materials with multivalent dopants via machine learning. *Chem. Eng. J.* **2023**, *452*, 139254. [CrossRef]
54. Kabra, V.; Birn, B.; Kamboj, I.; Augustyn, V.; Mukherjee, P.P. Mesoscale Machine Learning Analytics for Electrode Property Estimation. *J. Phys. Chem. C* **2022**, *126*, 14413–14429. [CrossRef]
55. Allam, O.; Kuramshin, R.; Stoichev, Z.; Cho, B.W.; Lee, S.W.; Jang, S.S. Molecular structure–redox potential relationship for organic electrode materials: Density functional theory–Machine learning approach. *Mater. Today Energy* **2020**, *17*, 100482. [CrossRef]
56. Li, W.; Zhang, J.; Ringbeck, F.; Jöst, D.; Zhang, L.; Wei, Z.; Sauer, D.U. Physics-informed neural networks for electrode-level state estimation in lithium-ion batteries. *J. Power Sources* **2021**, *506*, 230034. [CrossRef]
57. Bailey, J.J.; Wade, A.; Boyce, A.M.; Zhang, Y.S.; Brett, D.J.L.; Shearing, P.R. Quantitative assessment of machine-learning segmentation of battery electrode materials for active material quantification. *J. Power Sources* **2023**, *557*, 232503. [CrossRef]
58. Alfaruqi, M.H.; Lee, S.; Kang, H.; Sambandam, B.; Mathew, V.; Hwang, J.-Y.; Kim, J. Recent Achievements in Experimental and Computational Studies of Positive Electrode Materials for Nonaqueous Ca- and Al-Ion Batteries. *J. Phys. Chem. C* **2022**, *126*, 9209–9227. [CrossRef]

59. Faraji Niri, M.; Reynolds, C.; Román Ramírez, L.A.; Kendrick, E.; Marco, J. Systematic analysis of the impact of slurry coating on manufacture of Li-ion battery electrodes via explainable machine learning. *Energy Storage Mater.* **2022**, *51*, 223–238. [CrossRef]
60. Anniés, S.; Scheurer, C.; Panosetti, C. The intrinsic electrostatic dielectric behaviour of graphite anodes in Li-ion batteries—Across the entire functional range of charge. *Electrochim. Acta* **2023**, *444*, 141966. [CrossRef]
61. Jiao, J.; Lai, G.; Qin, S.; Fang, C.; Xu, X.; Jiang, Y.; Ouyang, C.; Zheng, J. Tuning of surface morphology in Li layered oxide cathode materials. *Acta Mater.* **2022**, *238*, 118229. [CrossRef]
62. Ellis, L.D.; Buteau, S.; Hames, S.G.; Thompson, L.M.; Hall, D.S.; Dahn, J.R. A New Method for Determining the Concentration of Electrolyte Components in Lithium-Ion Cells, Using Fourier Transform Infrared Spectroscopy and Machine Learning. *J. Electrochem. Soc.* **2018**, *165*, A256–A262. [CrossRef]
63. Zheng, Y.; Yao, Y.; Ou, J.; Li, M.; Luo, D.; Dou, H.; Li, Z.; Amine, K.; Yu, A.; Chen, Z. A review of composite solid-state electrolytes for lithium batteries: Fundamentals, key materials and advanced structures. *Chem. Soc. Rev.* **2020**, *49*, 8790–8839. [CrossRef] [PubMed]
64. Benayad, A.; Diddens, D.; Heuer, A.; Krishnamoorthy, A.N.; Maiti, M.; Le Cras, F.; Legallais, M.; Rahmanian, F.; Shin, Y.; Stein, H.; et al. High-Throughput Experimentation and Computational Freeway Lanes for Accelerated Battery Electrolyte and Interface Development Research. *Adv. Energy Mater.* **2022**, *12*, 210267. [CrossRef]
65. Yang, G.; Lehmann, M.L.; Zhao, S.; Li, B.; Ge, S.; Cao, P.-F.; Delnick, F.M.; Sokolov, A.P.; Saito, T.; Nanda, J. Anomalously high elastic modulus of a poly(ethylene oxide)-based composite electrolyte. *Energy Storage Mater.* **2021**, *35*, 431–442. [CrossRef]
66. Dave, A.; Mitchell, J.; Burke, S.; Lin, H.; Whitacre, J.; Viswanathan, V. Autonomous optimization of non-aqueous Li-ion battery electrolytes via robotic experimentation and machine learning coupling. *Nat. Commun.* **2022**, *13*, 5454. [CrossRef]
67. Sendek, A.D.; Antoniuk, E.R.; Cubuk, E.D.; Ransom, B.; Francisco, B.E.; Buettner-Garrett, J.; Cui, Y.; Reed, E.J. Combining Superionic Conduction and Favorable Decomposition Products in the Crystalline Lithium–Boron–Sulfur System: A New Mechanism for Stabilizing Solid Li-Ion Electrolytes. *ACS Appl. Mater. Interfaces* **2020**, *12*, 37957–37966. [CrossRef] [PubMed]
68. Kim, K.; Dive, A.; Grieder, A.; Adelstein, N.; Kang, S.; Wan, L.F.; Wood, B.C. Flexible machine-learning interatomic potential for simulating structural disordering behavior of Li7La3Zr2O12 solid electrolytes. *J. Chem. Phys.* **2022**, *156*, 221101. [CrossRef] [PubMed]
69. Dajnowicz, S.; Agarwal, G.; Stevenson, J.M.; Jacobson, L.D.; Ramezanghorbani, F.; Leswing, K.; Friesner, R.A.; Halls, M.D.; Abel, R. High-Dimensional Neural Network Potential for Liquid Electrolyte Simulations. *J. Phys. Chem. B* **2022**, *126*, 6271–6280. [CrossRef]
70. Adenusi, H.; Chass, G.A.; Passerini, S.; Tian, K.V.; Chen, G. Lithium Batteries and the Solid Electrolyte Interphase (SEI)—Progress and Outlook. *Adv. Energy Mater.* **2023**, *13*, 2203307. [CrossRef]
71. Shodiev, A.; Duquesnoy, M.; Arcelus, O.; Chouchane, M.; Li, J.; Franco, A.A. Machine learning 3D-resolved prediction of electrolyte infiltration in battery porous electrodes. *J. Power Sources* **2021**, *511*, 230384. [CrossRef]
72. Zhao, Y.; Schiffmann, N.; Koeppe, A.; Brandt, N.; Bucharsky, E.C.; Schell, K.G.; Selzer, M.; Nestler, B. Machine Learning Assisted Design of Experiments for Solid State Electrolyte Lithium Aluminum Titanium Phosphate. *Front. Mater.* **2022**, *9*, 821817. [CrossRef]
73. Ahmad, Z.; Xie, T.; Maheshwari, C.; Grossman, J.C.; Viswanathan, V. Machine Learning Enabled Computational Screening of Inorganic Solid Electrolytes for Suppression of Dendrite Formation in Lithium Metal Anodes. *ACS Cent. Sci.* **2018**, *4*, 996–1006. [CrossRef]
74. Satpati, A.; Kandregula, G.R.; Ramanujam, K. Machine learning enabled high-throughput screening of inorganic solid electrolytes for regulating dendritic growth in lithium metal anodes. *New J. Chem.* **2022**, *46*, 14227–14238. [CrossRef]
75. Kim, K.; Siegel, D.J. Machine learning reveals factors that control ion mobility in anti-perovskite solid electrolytes. *J. Mater. Chem. A* **2022**, *10*, 15169–15182. [CrossRef]
76. Duong, V.M.; Tran, T.N.; Garg, A.; Phung, T.G.; Tran, V.M.; Le, M.L.P.; Panwar, N.G. Machine learning technique-based data-driven model of exploring effects of electrolyte additives on LiNi0.6Mn0.2Co0.2O2/graphite cell. *J. Energy Storage* **2021**, *42*, 103012. [CrossRef]
77. Nakano, K.; Tanibata, N.; Takeda, H.; Kobayashi, R.; Nakayama, M.; Watanabe, N. Molecular Dynamics Simulation of Li-Ion Conduction at Grain Boundaries in NASICON-Type $LiZr_2(PO_4)_3$ Solid Electrolytes. *J. Phys. Chem. C* **2021**, *125*, 23604–23612. [CrossRef]
78. Sendek, A.D.; Cheon, G.; Pasta, M.; Reed, E.J. Quantifying the Search for Solid Li-Ion Electrolyte Materials by Anion: A Data-Driven Perspective. *J. Phys. Chem. C* **2020**, *124*, 8067–8079. [CrossRef]
79. Spotte-Smith, E.W.C.; Blau, S.M.; Xie, X.; Patel, H.D.; Wen, M.; Wood, B.; Dwaraknath, S.; Persson, K.A. Quantum chemical calculations of lithium-ion battery electrolyte and interphase species. *Sci. Data* **2021**, *8*, 203. [CrossRef] [PubMed]
80. Chen, W.; Li, Y.; Feng, D.; Lv, C.; Li, H.; Zhou, S.; Jiang, Q.; Yang, J.; Gao, Z.; He, Y.; et al. Recent progress of theoretical research on inorganic solid state electrolytes for Li metal batteries. *J. Power Sources* **2023**, *561*, 232720. [CrossRef]

81. Choi, E.; Jo, J.; Kim, W.; Min, K. Searching for Mechanically Superior Solid-State Electrolytes in Li-Ion Batteries via Data-Driven Approaches. *ACS Appl. Mater. Interfaces* **2021**, *13*, 42590–42597. [CrossRef] [PubMed]
82. Kumar, S.; Jaafreh, R.; Dutta, S.; Singh, S.N.; Hamad, K.; Ho Yoon, D. Introducing MagBERT: A language model for magnesium textual data mining and analysis. *J. Magnes. Alloys.* **2024**, *12*, 3216–3228. [CrossRef]
83. Fu, Z.-H.; Chen, X.; Yao, N.; Shen, X.; Ma, X.-X.; Feng, S.; Wang, S.; Zhang, R.; Zhang, L.; Zhang, Q. The chemical origin of temperature-dependent lithium-ion concerted diffusion in sulfide solid electrolyte Li10GeP2S12. *J. Energy Chem.* **2022**, *70*, 59–66. [CrossRef]
84. Wang, J.; Panchal, A.A.; Sai Gautam, G.; Canepa, P. The resistive nature of decomposing interfaces of solid electrolytes with alkali metal electrodes. *J. Mater. Chem. A* **2022**, *10*, 19732–19742. [CrossRef]
85. Lin, Y.-Y.; Yong, A.X.B.; Gustafson, W.J.; Reedy, C.N.; Ertekin, E.; Krogstad, J.A.; Perry, N.H. Toward design of cation transport in solid-state battery electrolytes: Structure-dynamics relationships. *Curr. Opin. Solid. State Mater. Sci.* **2020**, *24*, 100875. [CrossRef]
86. Hajibabaei, A.; Kim, K.S. Universal Machine Learning Interatomic Potentials: Surveying Solid Electrolytes. *J. Phys. Chem. Lett.* **2021**, *12*, 8115–8120. [CrossRef] [PubMed]
87. Wang, F.; Cheng, J. Unraveling the origin of reductive stability of super-concentrated electrolytes from first principles and unsupervised machine learning. *Chem. Sci.* **2022**, *13*, 11570–11576. [CrossRef]
88. Xiong, R.; Sun, Y.; Wang, C.; Tian, J.; Chen, X.; Li, H.; Zhang, Q. A data-driven method for extracting aging features to accurately predict the battery health. *Energy Storage Mater.* **2023**, *57*, 460–470. [CrossRef]
89. Pan, W.; Luo, X.; Zhu, M.; Ye, J.; Gong, L.; Qu, H. A health indicator extraction and optimization for capacity estimation of Li-ion battery using incremental capacity curves. *J. Energy Storage* **2021**, *42*, 103072. [CrossRef]
90. Gupta, Y. A Multi-Class Classification Based Approach for Remaining Useful Life (RUL) Prediction of Li-Ion Battery. *Biosci. Biotechnol. Res. Commun.* **2020**, *13*, 511–516. [CrossRef]
91. Wang, J.; Zhang, C.; Zhang, L.; Su, X.; Zhang, W.; Li, X.; Du, J. A novel aging characteristics-based feature engineering for battery state of health estimation. *Energy* **2023**, *273*, 127169. [CrossRef]
92. Lu, Y.; Maftouni, M.; Yang, T.; Zheng, P.; Young, D.; Kong, Z.J.; Li, Z. A novel disassembly process of end-of-life lithium-ion batteries enhanced by online sensing and machine learning techniques. *J. Intell. Manuf.* **2023**, *34*, 2463–2475. [CrossRef] [PubMed]
93. Pang, X.; Yang, W.; Wang, C.; Fan, H.; Wang, L.; Li, J.; Zhong, S.; Zheng, W.; Zou, H.; Chen, S.; et al. A novel hybrid model for lithium-ion batteries lifespan prediction with high accuracy and interpretability. *J. Energy Storage* **2023**, *61*, 106728. [CrossRef]
94. Patil, M.A.; Tagade, P.; Hariharan, K.S.; Kolake, S.M.; Song, T.; Yeo, T.; Doo, S. A novel multistage Support Vector Machine based approach for Li ion battery remaining useful life estimation. *Appl. Energy* **2015**, *159*, 285–297. [CrossRef]
95. Shu, X.; Li, G.; Shen, J.; Lei, Z.; Chen, Z.; Liu, Y. A uniform estimation framework for state of health of lithium-ion batteries considering feature extraction and parameters optimization. *Energy* **2020**, *204*, 117957. [CrossRef]
96. Faraji-Niri, M.; Rashid, M.; Sansom, J.; Sheikh, M.; Widanage, D.; Marco, J. Accelerated state of health estimation of second life lithium-ion batteries via electrochemical impedance spectroscopy tests and machine learning techniques. *J. Energy Storage* **2023**, *58*, 106295. [CrossRef]
97. Qu, W.; Li, J.; Zhang, R.; Liu, S.; Bao, J. Adaptive planning of human–robot collaborative disassembly for end-of-life lithium-ion batteries based on digital twin. *J. Intell. Manuf.* **2023**, *35*, 2021–2043. [CrossRef]
98. Gao, Y.; Li, C.; Huang, L. An improved deep extreme learning machine to predict the remaining useful life of lithium-ion battery. *Front. Energy Res.* **2022**, *10*, 1032660. [CrossRef]
99. Luo, W.; Syed, A.U.; Nicholls, J.R.; Gray, S. An SVM-Based Health Classifier for Offline Li-Ion Batteries by Using EIS Technology. *J. Electrochem. Soc.* **2023**, *170*, 030532. [CrossRef]
100. Mayilvahanan, K.S.; Takeuchi, K.J.; Takeuchi, E.S.; Marschilok, A.C.; West, A.C. Supervised Learning of Synthetic Big Data for Li-Ion Battery Degradation Diagnosis. *Batter Supercaps* **2022**, *5*, e202100166. [CrossRef]
101. Hosen, M.S.; Jaguemont, J.; Van Mierlo, J.; Berecibar, M. Battery lifetime prediction and performance assessment of different modeling approaches. *iScience* **2021**, *24*, 102060. [CrossRef] [PubMed]
102. Liu, X.; Zhang, L.; Yu, H.; Wang, J.; Li, J.; Yang, K.; Zhao, Y.; Wang, H.; Wu, B.; Brandon, N.P.; et al. Bridging Multiscale Characterization Technologies and Digital Modeling to Evaluate Lithium Battery Full Lifecycle. *Adv. Energy Mater.* **2022**, *12*, 2200889. [CrossRef]
103. Gasper, P.; Gering, K.; Dufek, E.; Smith, K. Challenging Practices of Algebraic Battery Life Models through Statistical Validation and Model Identification via Machine-Learning. *J. Electrochem. Soc.* **2021**, *168*, 020502. [CrossRef]
104. Su, L.; Wu, M.; Li, Z.; Zhang, J. Cycle life prediction of lithium-ion batteries based on data-driven methods. *eTransportation* **2021**, *10*, 100137. [CrossRef]
105. Li, R.; Hong, J.; Zhang, H.; Chen, X. Data-driven battery state of health estimation based on interval capacity for real-world electric vehicles. *Energy* **2022**, *257*, 124771. [CrossRef]
106. Severson, K.A.; Attia, P.M.; Jin, N.; Perkins, N.; Jiang, B.; Yang, Z.; Chen, M.H.; Aykol, M.; Herring, P.K.; Fraggedakis, D.; et al. Data-driven prediction of battery cycle life before capacity degradation. *Nat. Energy* **2019**, *4*, 383–391. [CrossRef]

107. Li, X.; Ju, L.; Geng, G.; Jiang, Q. Data-driven state-of-health estimation for lithium-ion battery based on aging features. *Energy* **2023**, *274*, 127378. [CrossRef]
108. Fei, Z.; Yang, F.; Tsui, K.-L.; Li, L.; Zhang, Z. Early prediction of battery lifetime via a machine learning based framework. *Energy* **2021**, *225*, 120205. [CrossRef]
109. Fei, Z.; Zhang, Z.; Yang, F.; Tsui, K.-L.; Li, L. Early-stage lifetime prediction for lithium-ion batteries: A deep learning framework jointly considering machine-learned and handcrafted data features. *J. Energy Storage* **2022**, *52*, 104936. [CrossRef]
110. Ran, A.; Liang, Z.; Chen, S.; Cheng, M.; Sun, C.; Ma, F.; Wang, K.; Li, B.; Zhou, G.; Zhang, X.; et al. Fast Clustering of Retired Lithium-Ion Batteries for Secondary Life with a Two-Step Learning Method. *ACS Energy Lett.* **2022**, *7*, 3817–3825. [CrossRef]
111. Li, A.G.; Wang, W.; West, A.C.; Preindl, M. Health and performance diagnostics in Li-ion batteries with pulse-injection-aided machine learning. *Appl. Energy* **2022**, *315*, 119005. [CrossRef]
112. Nuhic, A.; Terzimehic, T.; Soczka-Guth, T.; Buchholz, M.; Dietmayer, K. Health diagnosis and remaining useful life prognostics of lithium-ion batteries using data-driven methods. *J. Power Sources* **2013**, *239*, 680–688. [CrossRef]
113. Maleki, S.; Ray, B.; Hagh, M.T. Hybrid framework for predicting and forecasting State of Health of Lithium-ion batteries in Electric Vehicles. *Sustain. Energy Grids Netw.* **2022**, *30*, 100603. [CrossRef]
114. Zhang, Y.; Tang, Q.; Zhang, Y.; Wang, J.; Stimming, U.; Lee, A.A. Identifying degradation patterns of lithium ion batteries from impedance spectroscopy using machine learning. *Nat. Commun.* **2020**, *11*, 1706. [CrossRef]
115. Zhang, C.; Wang, S.; Yu, C.; Xie, Y.; Fernandez, C. Improved Particle Swarm Optimization-Extreme Learning Machine Modeling Strategies for the Accurate Lithium-ion Battery State of Health Estimation and High-adaptability Remaining Useful Life Prediction. *J. Electrochem. Soc.* **2022**, *169*, 080520. [CrossRef]
116. Thelen, A.; Lui, Y.H.; Shen, S.; Laflamme, S.; Hu, S.; Ye, H.; Hu, C. Integrating physics-based modeling and machine learning for degradation diagnostics of lithium-ion batteries. *Energy Storage Mater.* **2022**, *50*, 668–695. [CrossRef]
117. Smith, K.; Gasper, P.; Colclasure, A.M.; Shimonishi, Y.; Yoshida, S. Lithium-Ion Battery Life Model with Electrode Cracking and Early-Life Break-in Processes. *J. Electrochem. Soc.* **2021**, *168*, 100530. [CrossRef]
118. Rauf, H.; Khalid, M.; Arshad, N. Machine learning in state of health and remaining useful life estimation: Theoretical and technological development in battery degradation modelling. *Renew. Sustain. Energy Rev.* **2022**, *156*, 111903. [CrossRef]
119. Chen, Z.; Shi, N.; Ji, Y.; Niu, M.; Wang, Y. Lithium-ion batteries remaining useful life prediction based on BLS-RVM. *Energy* **2021**, *234*, 121269. [CrossRef]
120. Rouhi Ardeshiri, R.; Ma, C. Multivariate gated recurrent unit for battery remaining useful life prediction: A deep learning approach. *Int. J. Energy Res.* **2021**, *45*, 16633–16648. [CrossRef]
121. Pan, H.; Lü, Z.; Wang, H.; Wei, H.; Chen, L. Novel battery state-of-health online estimation method using multiple health indicators and an extreme learning machine. *Energy* **2018**, *160*, 466–477. [CrossRef]
122. Shu, X.; Li, G.; Zhang, Y.; Shen, J.; Chen, Z.; Liu, Y. Online diagnosis of state of health for lithium-ion batteries based on short-term charging profiles. *J. Power Sources* **2020**, *471*, 228478. [CrossRef]
123. Wang, H.; Li, J.; Liu, X.; Rao, J.; Fan, Y.; Tan, X. Online state of health estimation for lithium-ion batteries based on a dual self-attention multivariate time series prediction network. *Energy Rep.* **2022**, *8*, 8953–8964. [CrossRef]
124. Chen, Z.; Zhang, S.; Shi, N.; Li, F.; Wang, Y.; Cui, J. Online state-of-health estimation of lithium-ion battery based on relevance vector machine with dynamic integration. *Appl. Soft Comput.* **2022**, *129*, 109615. [CrossRef]
125. Greenbank, S.; Howey, D.A. Piecewise-linear modelling with automated feature selection for Li-ion battery end-of-life prognosis. *Mech. Syst. Signal Process.* **2023**, *184*, 109612. [CrossRef]
126. Xu, S.; Zha, F.-L.; Huang, B.-W.; Yu, B.; Huang, H.-B.; Zhou, T.; Mao, W.-Q.; Wu, J.-J.; Wei, J.-Q.; Gong, S.-K.; et al. Research on the state of health estimation of lithium-ion batteries for energy storage based on XGB-AKF method. *Front. Energy Res.* **2023**, *10*, 999676. [CrossRef]
127. Shah, A.; Shah, K.; Shah, C.; Shah, M. State of charge, remaining useful life and knee point estimation based on artificial intelligence and Machine learning in lithium-ion EV batteries: A comprehensive review. *Renew. Energy Focus* **2022**, *42*, 146–164. [CrossRef]
128. Li, R.; Li, W.; Zhang, H. State of Health and Charge Estimation Based on Adaptive Boosting integrated with particle swarm optimization/support vector machine (AdaBoost-PSO-SVM) Model for Lithium-ion Batteries. *Int. J. Electrochem. Sci.* **2022**, *17*, 220212. [CrossRef]
129. Shu, X.; Shen, S.; Shen, J.; Zhang, Y.; Li, G.; Chen, Z.; Liu, Y. State of health prediction of lithium-ion batteries based on machine learning: Advances and perspectives. *iScience* **2021**, *24*, 103265. [CrossRef]
130. Lee, G.; Kim, J.; Lee, C. State-of-health estimation of Li-ion batteries in the early phases of qualification tests: An interpretable machine learning approach. *Expert Syst. Appl.* **2022**, *197*, 116817. [CrossRef]
131. Mawonou, K.S.R.; Eddahech, A.; Dumur, D.; Beauvois, D.; Godoy, E. State-of-health estimators coupled to a random forest approach for lithium-ion battery aging factor ranking. *J. Power Sources* **2021**, *484*, 229154. [CrossRef]

132. Li, G.; Li, B.; Li, C.; Wang, S. State-of-health rapid estimation for lithium-ion battery based on an interpretable stacking ensemble model with short-term voltage profiles. *Energy* **2023**, *263*, 126064. [CrossRef]
133. Attia, P.M.; Severson, K.A.; Witmer, J.D. Statistical Learning for Accurate and Interpretable Battery Lifetime Prediction. *J. Electrochem. Soc.* **2021**, *168*, 090547. [CrossRef]
134. Lyu, Z.; Wang, G.; Gao, R. Synchronous state of health estimation and remaining useful lifetime prediction of Li-Ion battery through optimized relevance vector machine framework. *Energy* **2022**, *251*, 123852. [CrossRef]
135. Li, A.G.; West, A.C.; Preindl, M. Towards unified machine learning characterization of lithium-ion battery degradation across multiple levels: A critical review. *Appl. Energy* **2022**, *316*, 119030. [CrossRef]
136. Zhang, Z.; Mansouri Tehrani, A.; Oliynyk, A.O.; Day, B.; Brgoch, J. Finding the Next Superhard Material through Ensemble Learning. *Adv. Mater.* **2021**, *33*, 2005112. [CrossRef]
137. Jaafreh, R.; Sharan, A.; Sajjad, M.; Singh, N.; Hamad, K. A Machine Learning-Assisted Approach to a Rapid and Reliable Screening for Mechanically Stable Perovskite-Based Materials. *Adv. Funct. Mater.* **2023**, *33*, 2210374. [CrossRef]
138. Jaafreh, R.; Kang, Y.S.; Hamad, K. Brittle and ductile characteristics of intermetallic compounds in magnesium alloys: A large-scale screening guided by machine learning. *J. Magnes. Alloys* **2023**, *11*, 392–404. [CrossRef]
139. Xue, D.; Xue, D.; Yuan, R.; Zhou, Y.; Balachandran, P.V.; Ding, X.; Sun, J.; Lookman, T. An informatics approach to transformation temperatures of NiTi-based shape memory alloys. *Acta Mater.* **2017**, *125*, 532–541. [CrossRef]
140. Jaafreh, R.; Chaudry, U.M.; Hamad, K.; Abuhmed, T. Age-hardening behavior guided by the multi-objective evolutionary algorithm and machine learning. *J. Alloys Compd.* **2022**, *893*, 162104. [CrossRef]
141. Van Setten, M.J.; Dekkers, H.F.W.; Pashartis, C.; Chasin, A.; Belmonte, A.; Delhougne, R.; Kar, G.S.; Pourtois, G. Complex amorphous oxides: Property prediction from high throughput DFT and AI for new material search. *Mater. Adv.* **2022**, *3*, 8413–8427. [CrossRef]
142. Lu, W.-C.; Ji, X.-B.; Li, M.-J.; Liu, L.; Yue, B.-H.; Zhang, L.-M. Using support vector machine for materials design. *Adv. Manuf.* **2013**, *1*, 151–159. [CrossRef]
143. Kurban, H.; Kurban, M. Building Machine Learning systems for multi-atoms structures: CH3NH3PbI3 perovskite nanoparticles. *Comput. Mater. Sci.* **2021**, *195*, 110490. [CrossRef]
144. Jaafreh, R.; Kang, Y.S.; Hamad, K. Lattice Thermal Conductivity: An Accelerated Discovery Guided by Machine Learning. *ACS Appl. Mater. Interfaces* **2021**, *13*, 57204–57213. [CrossRef]
145. Jaafreh, R.; Kang, Y.S.; Kim, J.G.; Hamad, K. Machine learning guided discovery of super-hard high entropy ceramics. *Mater Lett.* **2022**, *306*, 130899. [CrossRef]
146. Deringer, V.L.; Bartók, A.P.; Bernstein, N.; Wilkins, D.M.; Ceriotti, M.; Csányi, G. Gaussian Process Regression for Materials and Molecules. *Chem. Rev.* **2021**, *121*, 10073–10141. [CrossRef]
147. Pereznieto, S.; Jaafreh, R.; Kim, J.; Hamad, K. Solid electrolytes for Li-ion batteries via machine learning. *Mater. Lett.* **2023**, *337*, 133926. [CrossRef]
148. Kumar, S.; Jaafreh, R.; Dutta, S.; Pereznieto, S.; Hamad, K.; Ho Yoon, D. Learning techniques for designing solid-state lithium-ion batteries with high thermomechanical stability. *Mater. Lett.* **2023**, *351*, 135049. [CrossRef]
149. Kim, E.; Huang, K.; Saunders, A.; McCallum, A.; Ceder, G.; Olivetti, E. Materials Synthesis Insights from Scientific Literature via Text Extraction and Machine Learning. *Chem. Mater.* **2017**, *29*, 9436–9444. [CrossRef]
150. Mahbub, R.; Huang, K.; Jensen, Z.; Hood, Z.D.; Rupp, J.L.M.; Olivetti, E.A. Text mining for processing conditions of solid-state battery electrolytes. *Electrochem. Commun.* **2020**, *121*, 106860. [CrossRef]

Disclaimer/Publisher's Note: The statements, opinions and data contained in all publications are solely those of the individual author(s) and contributor(s) and not of MDPI and/or the editor(s). MDPI and/or the editor(s) disclaim responsibility for any injury to people or property resulting from any ideas, methods, instructions or products referred to in the content.